Human Molecular Genetics, 2013, Vol. 22, No. 8 **1643–1653**
doi:10.1093/hmg/ddt014
Advance Access published on January 17, 2013

Functional analysis of a duplication (p.E63_D69dup) in the switch II region of HRAS: new aspects of the molecular pathogenesis underlying Costello syndrome

Sybille Lorenz[1], Christina Lissewski[2], Pelin O. Simsek-Kiper[3], Yasemin Alanay[4], Koray Boduroglu[3], Martin Zenker[2,*] and Georg Rosenberger[1,*]

[1]Institute of Human Genetics, University Medical Center Hamburg-Eppendorf, Hamburg 20246, Germany, [2]Institute of Human Genetics, University Hospital Magdeburg, Magdeburg 39120, Germany, [3]Clinical Genetics Unit, İhsan Doğramacı Children's Hospital, Hacettepe University, Ankara 06100, Turkey and [4]Pediatric Genetics Unit, Department of Pediatrics, Faculty of Medicine, Acibadem University, Istanbul 34848, Turkey

Received November 21, 2012; Revised and Accepted January 14, 2013

Costello syndrome is a congenital disorder comprising a characteristic face, severe feeding difficulties, skeletal, cardiac and skin abnormalities, intellectual disability and predisposition to malignancies. It is caused by heterozygous germline *HRAS* mutations mostly affecting Gly^{12} or Gly^{13}, which impair HRAS-GTPase activity and result in increased downstream signal flow independent of incoming signals. Functional analyses of rarer *HRAS* mutations identified in individuals with attenuated Costello syndrome phenotypes revealed altered GDP/GTP nucleotide affinities (p.K117R) and inefficient effector binding (p.E37dup). Thus, both phenotypic and functional variability associated with *HRAS* mutations are evident. Here, we report on a novel heterozygous *HRAS* germline mutation (c.187_207dup, p.E63_D69dup) in a girl presenting with a phenotype at the milder end of the Costello syndrome spectrum. The p.E63_D69dup mutation impaired co-precipitation of recombinant HRAS with NF1 GTPase-activating protein (GAP) suggesting constitutive $HRAS^{E63\_D69dup}$ activation due to GAP insensitivity. Indeed, we identified strongly augmented active $HRAS^{E63\_D69dup}$ that co-precipitated with effectors RAF1, RAL guanine nucleotide dissociation stimulator and phospholipase C1. However, we could not pull down active $HRAS^{E63\_D69dup}$ using the target protein PIK3CA, indicating a compromised association between active $HRAS^{E63\_D69dup}$ and PIK3CA. Accordingly, overexpression of $HRAS^{E63\_D69dup}$ increased steady-state phosphorylation of MEK1/2 and ERK1/2 downstream of RAF, whereas AKT phosphorylation downstream of phosphoinositide 3-kinase (PI3K) was not enhanced. By analyzing signaling dynamics, we found that $HRAS^{E63\_D69dup}$ has impaired reagibility to stimuli resulting in reduced and disrupted capacity to transduce incoming signals to the RAF-MAPK and PI3K-AKT cascade, respectively. We suggest that disrupted HRAS reagibility, as we demonstrate for the p.E63_D69dup mutation, is a previously unappreciated molecular pathomechanism underlying Costello syndrome.

INTRODUCTION

Costello syndrome (OMIM #218040) is characterized by severe feeding problems in infancy, short stature, coarse facial features with full lips and a large mouth, curly or sparse, fine hair, cardiac abnormalities, including tachyarrhythmia and hypertrophic cardiomyopathy, a predisposition to papillomata and malignant tumors, as well as neurologic

*To whom correspondence should be addressed at: Institute of Human Genetics, University Hospital Magdeburg, Leipziger St. 44, Magdeburg 39120, Germany. Tel: +49 3916715064; Fax: +49 3916715066; Email: martin.zenker@med.ovgu.de (M.Z.); Institute of Human Genetics, University Medical Center Hamburg-Eppendorf, Martinistraße 52, Hamburg 20246, Germany. Tel: +49 40741054534; Fax: +49 40741055138; Email: rosenberger@uke.de (G.R.).

abnormalities, including intellectual disability, nystagmus and hypotonia (1). Heterozygous germline mutations in the proto-oncogene *HRAS* underlie Costello syndrome (2).

HRAS serves as signal transducer by alternating between an active guanosine triphosphate (GTP)-bound and inactive guanosine diphosphate (GDP)-bound state. The kinetics of GDP dissociation and GTP hydrolysis are modulated by two classes of proteins: Guanine nucleotide exchange factors (GEFs) activate HRAS by mediating the exchange of GDP for GTP, whereas GTPase-activating proteins (GAPs) stimulate the low intrinsic GTPase activity, thereby negatively controlling RAS function (3,4). In the active state, HRAS binds to a number of effector proteins, such as serine/threonine RAF kinases, the catalytic subunits of phosphoinositide 3-kinase (PI3K), phospholipase C1 (PLCE1) and RAL guanine nucleotide dissociation stimulator (RALGDS) (5). As a result, signal flow via these HRAS target proteins is increased.

More than 80% of patients with Costello syndrome share the same *HRAS* mutation, c.34G>A (p.G12S), that is associated with the typical and relatively homogeneous phenotype (6,7). The functional consequences of mutations of HRAS amino acid 12 were extensively studied due to their prominent role in oncogenic transformation. Such alterations affect intrinsic and GAP-stimulated hydrolytic activity of HRAS and thus maintain the active form and decouple HRAS from incoming signals (8–11). Therefore, 'gain-of-function' and 'hyperactivation' concerning HRAS downstream signaling pathways are widely accepted as the molecular basis of Costello syndrome. Functional characterization of rarer HRAS germline mutations, however, revealed additional molecular consequences/pathomechanisms, including altered GDP/GTP nucleotide affinities (p.K117R) (12) and inefficient effector binding (p.E37dup) (13). Such rare *HRAS* germline mutations have been reported in individuals with attenuated phenotypes (p.T58I, p.K117R, pA146T, p.A146V and p.E37dup) (12–16) or congenital myopathy and variable features resembling Costello syndrome (p.Q22K and p.E63K) (17). Furthermore, individuals with Costello syndrome and HRAS amino acid change p.G13C show distinctive ectodermal findings (18). Given the available data, further expansion of the phenotypic and functional variability associated with *HRAS* germline mutations has been proposed (19,20).

To attain a comprehensive picture of the phenotypic and functional variability, it is important both to delineate the clinical findings and to determine the functional consequences for novel *HRAS* sequence changes. Even if it is impossible to draw genotype–phenotype conclusions based on single patients, functional analyses will help to understand the underlying molecular deficiencies, thereby, providing a rational basis for possible therapeutic options. Here, we further document the broad phenotypic and functional variability associated with HRAS mutations by characterizing the novel HRAS p.E63_D69dup mutation.

RESULTS

Identification of a novel heterozygous *HRAS* mutation in a girl with clinical characteristics of Costello syndrome

The patient's clinical manifestations prompted the clinical diagnosis of Costello syndrome (Fig. 1A). However, her phenotype was considered to represent the milder end of the clinical spectrum for this condition based on her relatively mild feeding problems and intellectual impairment. We detected the novel heterozygous 21 bp duplication c.187_207dup in exon 3 of *HRAS* in the patient's DNA (Data not shown). Genotyping of parental DNAs did not identify this alteration and confirmed paternity, indicating *de novo* occurrence of the *HRAS* c.187_207dup mutation (Data not shown). The *HRAS* c.187_207dup mutation was predicted to cause duplication of HRAS amino acids 63–69 (p.E63_D69dup) (Fig. 1B). Five of these residues are integral part of the HRAS switch II domain (amino acids 59–67) that mediates binding of HRAS with various regulator and effector proteins (Fig. 1B) (10,21–24). Of note, the p.E63_D69dup mutation represents the first germline molecular lesion affecting more than one amino acid in HRAS and, thereby, might exert strong impact on HRAS protein structure.

The p.E63_D69dup mutation increases HRAS co-precipitation with effector proteins RAF1, RALGDS and PLCE1, but not with PIK3CA *in vivo*

To explore the molecular consequences of the p.E63_D69dup mutation, we precipitated activated hemagglutinin (HA)-tagged HRAS protein variants from COS-7 cell extracts using glutathione S-transferase (GST)-fusion proteins of interacting motifs from various RAS effectors. Co-precipitation of HA-HRAS^{G12S} and HA-HRAS^{G12V} with any tested effector was strongly enhanced under steady-state cell culture conditions, including serum starvation (0.1% serum) and basal growth condition (10% serum) when compared with HA-HRAS^{WT} (Fig. 2A and B). In contrast, the dominant negative mutant HA-HRAS^{S17N} (25,26) was not pulled down efficiently (Fig. 2A and B). The amount of HA-HRAS^{E63_D69dup} was similar to that of HA-HRAS^{G12S} or HA-HRAS^{G12V} in the RAF1, PLCE1 and RALGDS precipitates under serum-starved and basal conditions (Fig. 2A and B). However, it was decreased when compared with HA-HRAS^{WT} in precipitates using PIK3CA as bait (Fig. 2A and B). These data suggest (i) that HA-HRAS^{E63_D69dup} is trapped in an active conformation resulting in stabile binding to RAF1, PLCE1 and RALGDS and (ii) that the p.E63_D69dup mutation negatively affects binding to PIK3CA.

p.E63_D69dup affects HRAS interaction with NF1 GAP

HRAS has a low intrinsic GTPase activity that is dramatically stimulated by GAPs, and the switch II region is critical for GAP binding (10,27,28). Thus, increased activation of HA-HRAS^{E63_D69dup} as suggested by Figure 2 may result from impaired GAP interaction. To analyze binding of the RAS-specific NF1 GAP, we co-expressed the GAP-related domain of NF1, called NF1^{333}, together with HRAS protein variants in COS-7 cells and performed co-immunoprecipitation experiments. FLAG-tagged NF1^{333} strongly co-precipitated with constitutively active HA-HRAS^{G12V} or HA-HRAS^{G12S}, but not with dominant negative HA-HRAS^{S17N} (Fig. 3). We could also pull down FLAG-NF1^{333} together with HA-HRAS^{WT}, most likely reflecting the fraction of active HA-HRAS^{WT} molecules in the cell lysates (Fig. 3). In contrast, FLAG-NF1^{333} did

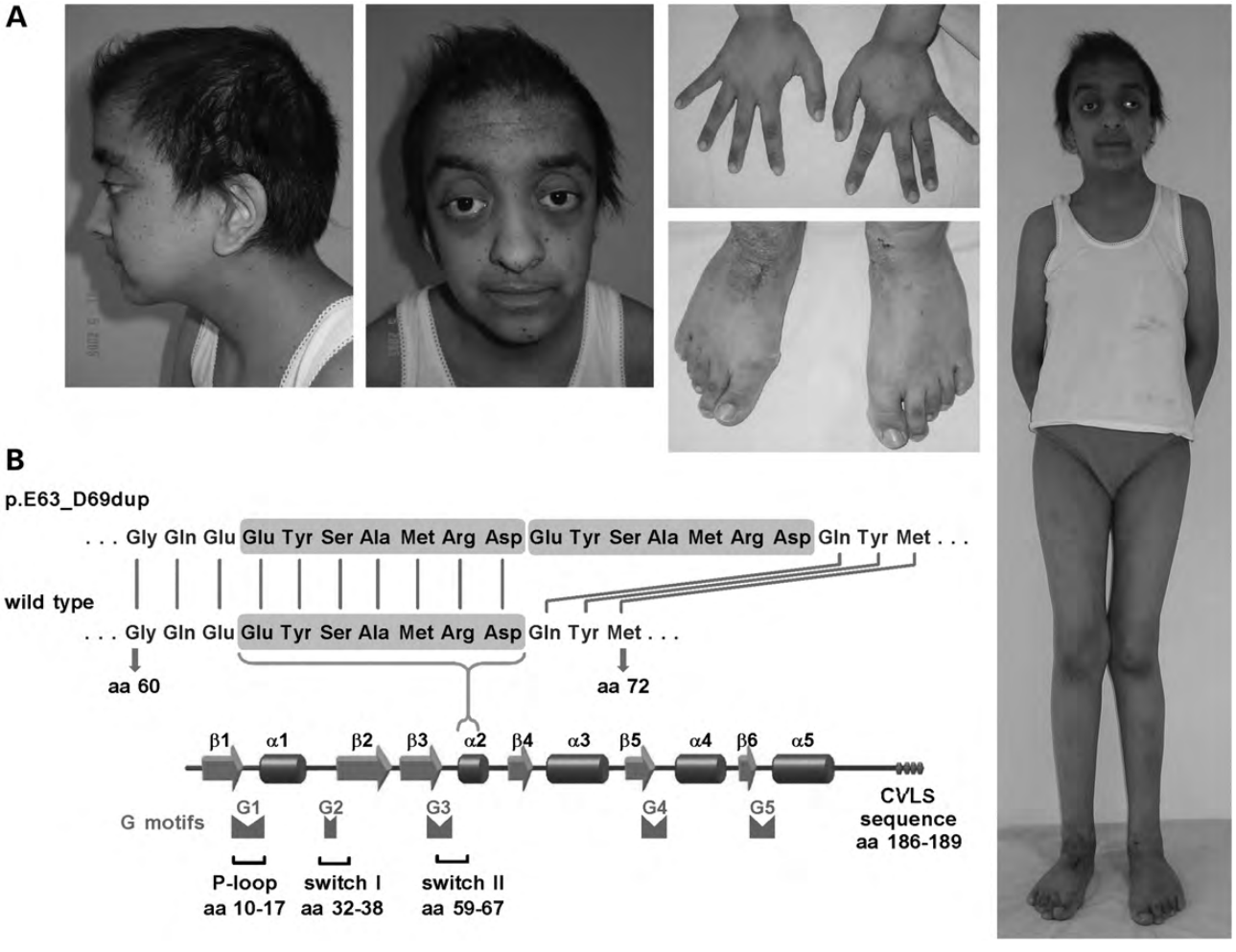

Figure 1. *HRAS* c.187_207dup (p.E63_D69dup) is associated with Costello syndrome. (**A**) Photographs of the patient at age 13 years. Note the typical facial features of a RASopathy, prematurely aged appearance, sparse hair and hyperkeratotic skin lesions at the ankles. (**B**) Position of amino acids 63–69 within the secondary structure of the HRAS GTPase. Secondary structural elements are shown as arrows and cylinders representing β-sheets and α-helices, respectively. Motifs representing the P-loop and switch I and II regions are indicated below the protein structure; amino acids (aa) constituting these motifs are given. The C-terminus of HRAS contains the membrane-targeting CVLS (Cys-Val-Leu-Ser) motif. HRAS has five conserved G motifs (G1–G5, gray boxes) (56). Amino acids 63–69 and duplicated residues are highlighted above the HRAS structure by gray background.

not considerably co-precipitate with HA-HRAS^{E63_D69dup} (Fig. 3) which indicates that duplication of amino acids 63–69 in HRAS interferes with NF1 GAP binding.

HRAS^{E63_D69dup} increases phosphorylation of MEK1/2 and ERK1/2

To gain insight into the consequences of the p.E63_D69dup mutation on HRAS-dependent downstream signaling, we determined levels of phosphorylated MEK1/2, ERK1/2 and AKT in COS-7 cells ectopically expressing HA-tagged HRAS protein variants. Whereas the dominant negative mutant HA-HRAS^{S17N} induced only very weak downstream signaling (Fig. 4A and B), HA-HRAS^{G12V} and HA-HRAS^{G12S} were found to markedly stimulate MEK1/2, ERK1/2 and AKT phosphorylation both under serum-starved (Fig. 4A) and basal (Fig. 4B) conditions. Similarly, HA-HRAS^{E63_D69dup} induced increased phosphorylation of downstream effectors under steady-state culture conditions when compared with HA-HRAS^{WT} (Fig. 4A and B). In detail, the hyperactivation was more pronounced for MEK1/2 and ERK1/2 than for AKT (Fig. 4A and B). Together, the data suggest that p.E63_D69dup preferentially intensifies mitogen-activated protein kinase (MAPK) signal flux.

HRAS^{E63_D69dup} shows residual reagibility to stimuli

Experiments with steady-state cell cultures are not informative concerning signaling dynamics. Therefore, we analyzed the intensity of downstream signaling upon epidermal growth factor (EGF) stimulation in transiently transfected COS-7 cultures. Serum-starved cells expressing HA-HRAS^{WT} had low levels of phosphorylated MEK1/2, ERK1/2 and AKT that all increased markedly 10 min after EGF stimulation (Fig. 5A). In contrast, expression of HA-HRAS^{G12V} resulted in robust basal phosphorylation of MEK1/2, ERK1/2 and AKT even in starved cells and only moderate or no augmentation in response to EGF stimulation; the small increment in pMEK and pERK may, at least in part, derive from untransfected cells (Fig. 5A). In

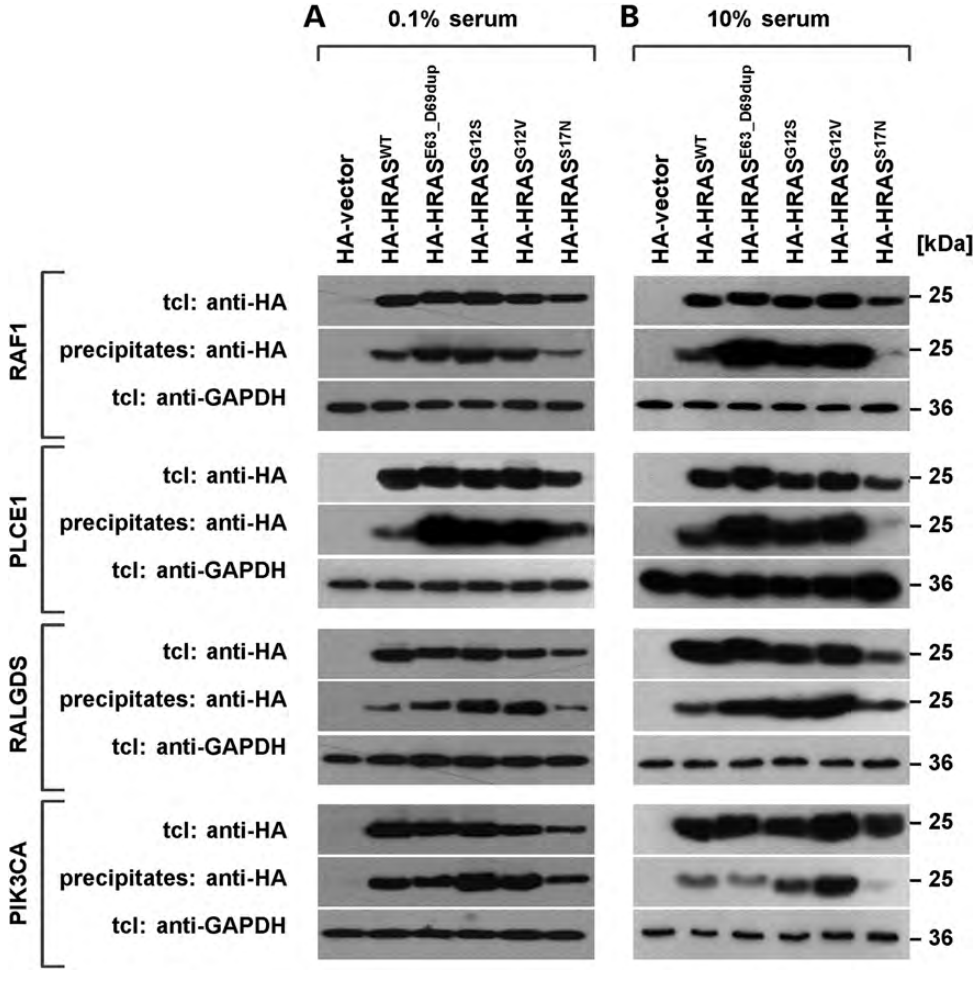

Figure 2. $HRAS^{E63\_D69dup}$ co-precipitates with RAF1, RALGDS and PLCE1, but not with PIK3CA. COS-7 cells transiently expressing HA-$HRAS^{WT}$ (wild-type), HA-$HRAS^{E63\_D69dup}$, HA-$HRAS^{G12S}$, HA-$HRAS^{G12V}$ or HA-$HRAS^{S17N}$ were cultured under serum-starved [0.1% serum, (A)] or basal [10% serum, (B)] growth conditions. GTP-bound HA-tagged HRAS protein variants were precipitated from cell extracts using GST-RAF1:RBD, GST-PLCE1:RA, GST-RALGDS:RA or GST-PIK3CA:RBD fusion proteins as indicated (RBD, RAS binding domain; RA, RAS association domain). Vector controls are shown in the first lane each. Precipitated HA-HRAS (precipitates) and total amounts of HA-HRAS proteins in the cellular extracts (tcl) were detected by immunoblotting using anti-HA antibody. Cellular extracts were probed with anti-GAPDH antibody to control for equal loading. Representative blots from three independent experiments are shown. tcl, total cell lysates.

HA-$HRAS^{E63\_D69dup}$ expressing cells, we found elevated phosphorylation levels at baseline (0 min) and hence a reduced phosphorylation response (10 min EGF stimulation) of MEK1/2 and ERK1/2 when compared with cells expressing HA-$HRAS^{WT}$ (Fig. 5A). AKT phosphorylation did not show any increase upon EGF stimulation in cells expressing HA-$HRAS^{E63\_D69dup}$ (Fig. 5A). This suggests that expression of $HRAS^{E63\_D69dup}$ seems to partially retain MAPK signaling sensitivity upon EGF stimulation, which is unlike constitutive active HA-$HRAS^{G12V}$.

To examine signaling dynamics in detail, we determined EGF response over time and statistically evaluated densitometric measurements of autoradiographs. Following EGF treatment, we detected strong activation of HA-$HRAS^{WT}$ and to a lesser extent of HA-$HRAS^{E63\_D69dup}$ (Fig. 5B, Panels 1 and 2); EGF stimulation resulted in an increase in active HA-$HRAS^{WT}$ by 56% (from 44% at 0 min EGF to maximum activation of 100% after 15 min EGF), whereas activation of HA-$HRAS^{E63\_D69dup}$ was enhanced only by 32% (from 68% at 0 min EGF to maximum activation of 100% after 15 min EGF) (Fig. 5C, top graph). In contrast, EGF had no effect on the activation of constitutively active HA-$HRAS^{G12V}$ (Fig. 5B and C). The phosphorylation levels of HRAS effectors MEK1/2 and ERK1/2 correlated well with the amounts of active HRAS (Fig. 5B, Panels 3–6); EGF stimulation induced a strong phosphorylation response in HA-$HRAS^{WT}$ cells, whereas in cells expressing $HRAS^{G12V}$, there was only little further increment. The residual activation in the latter case most likely originates from untransfected cells in the cultures. EGF-induced phosphorylation increment of MEK1/2 and ERK1/2 in cells expressing HA-$HRAS^{E63\_D69dup}$ was weaker than in $HRAS^{WT}$ cells, but significantly stronger than in $HRAS^{G12V}$ cells (Fig. 5C, second and third graph). This suggests that $HRAS^{E63\_D69dup}$ is able to transmit EGF stimulation to MAPK signaling cascades with an efficiency that is in between that of $HRAS^{WT}$ and $HRAS^{G12V}$. AKT phosphorylation, however, only marginally increased upon EGF treatment in cells expressing

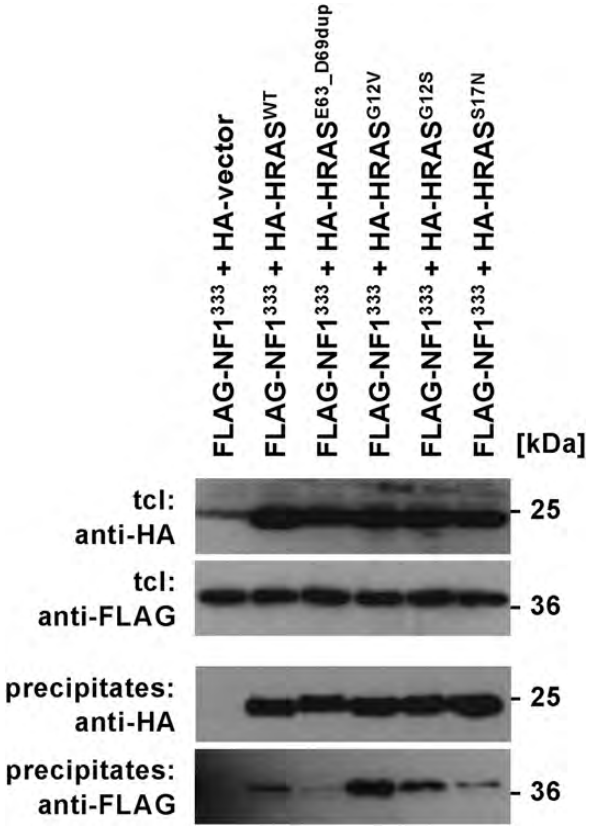

Figure 3. The p.E63_D69 mutation impairs binding of NF1 GAP. COS-7 cells were transfected with expression constructs as indicated and cultured under basal growth conditions (10% serum). Vector control is shown in lane 1. HA-tagged HRAS protein variants were immunoprecipitated from cell extracts using anti-HA-conjugated agarose beads. Upon SDS PAGE and western blotting, precipitates and total cell lysates (tcl) were probed with anti-HA and anti-FLAG antibodies.

$HRAS^{E63\_D69dup}$ (Fig. 5B, Panels 7 and 8). This was very similar to $HRAS^{G12V}$ cells, but not to $HRAS^{WT}$ transfected cultures that showed a strong AKT phosphorylation response upon EGF stimulation (Fig. 5B and C). This finding is in line with the observation of a reduced interaction of $HRAS^{E63\_D69dup}$ with the AKT upstream regulator subunit PIK3CA (Fig. 2).

Taken together, our data suggest that in addition to restricting PI3K binding, the p.E63_D69dup mutation moderately increases HRAS basal activation, resulting in a limited capacity to modulate signaling.

DISCUSSION

The functional analysis of rare Costello syndrome-associated HRAS mutations can improve the understanding of the molecular deficiencies underlying this disorder. With the identification and characterization of the p.E63_D69 mutation here, we add novel aspects to the knowledge of HRAS dysfunction and shift the focus from harmful HRAS hyperactivation toward pathologic hyporeagibility to stimuli.

Functional consequences

HRAS mutations that cause Costello syndrome are associated with increased HRAS activation and enhanced RAF-MAPK and/or PI3K-AKT signal flow (5,12,14,16,17,29). Using RAF1, PLCE1 or RALGDS in cellular GTPase activation assays, we could co-precipitate increased amounts of $HRAS^{E63\_D69dup}$ from cell extracts (Fig. 2); this suggests that the p.E63_D69dup mutation results in hyperactivation of HRAS that is generally in line with the effects of other Costello syndrome-associated HRAS mutations. Notably, we detected increased amounts of active $HRAS^{E63\_D69dup}$ both under serum-starved and basal conditions (Fig. 2). Thus, activation of $HRAS^{E63\_D69dup}$ does not depend on serum factors, and, therefore, $HRAS^{E63\_D69dup}$ may represent a constitutive active HRAS variant similar to $HRAS^{K117R}$, $HRAS^{G12V}$ and $HRAS^{G12S}$ that do not depend on growth factors to exert their activating potential (12,29).

Amino acids 63–69 constitute integral components of the highly mobile switch II region (Fig. 1B) that is involved in binding regulator proteins, including GAPs, GEFs and GDP dissociation inhibitors as well as effector molecules and GDP/GTP nucleotides (10,21–24). Here, we demonstrate impaired binding of $HRAS^{E63\_D69dup}$ with NF1 GAP (Fig. 3), suggesting that the p.E63_D69dup mutation strongly interferes with the structure of the switch II region that is critical for interaction with GAPs such as NF1 and p120GAP (10,27,28). Recently, altered GAP binding has been shown for another Costello syndrome-associated HRAS change, the duplication of glutamic acid at position 37 ($HRAS^{E37dup}$) in the switch I region of HRAS (13). Our data indicate that, similar to the $HRAS^{E37dup}$ mutant, $HRAS^{E63\_D69dup}$ accumulates in the GTP-bound form due to substantially reduced GAP affinity.

We could not co-precipitate $HRAS^{E63\_D69dup}$ using PIK3CA, the catalytic subunit of PI3K (Fig. 2), that makes critical interactions with the switch II region (30,31). Similarly, substitution of HRAS tyrosine 64 by a glycine eliminated the interaction with PI3K and also with NF1, whereas this substitution had no effect on RAF1 binding (32). Indeed, the effector proteins RAF1 and RALGDS interact with switch I, but not switch II of RAS (21). PLCE1 is able to make contact with both switch I and switch II, thereby, sharing this ability with PI3K (33). Assuming a distorted structure of the $HRAS^{E63\_D69dup}$ switch II region, our results indicate that PLCE1 interaction with switch I is sufficient for effective binding (Fig. 2). Thus, p.E63_D69dup may specifically impair interaction with PIK3CA, but not with RAF1, RALGDS and PLCE1.

In line with the results derived from GTPase activation assays, $HRAS^{E63\_D69dup}$ induced strong phosphorylation of RAF1 downstream effectors MEK1/2 and ERK1/2 both under serum-starved and basal conditions (Fig. 4), suggesting a constitutive activating effect of the p.E63_D69dup mutation. On the contrary, phospho-AKT was found to be only marginally elevated in cells expressing $HRAS^{E63\_D69dup}$ (Fig. 4), a consequence obviously originating from impaired PI3K binding to activated $HRAS^{E63\_D69dup}$. Costello syndrome-associated HRAS mutations exert their pathogenic consequences by gain-of-function of HRAS-dependent signal transduction resulting in enhanced RAF1-MEK-ERK and PI3K-AKT signal flux (12,34). The p.E63_D69dup mutation, however,

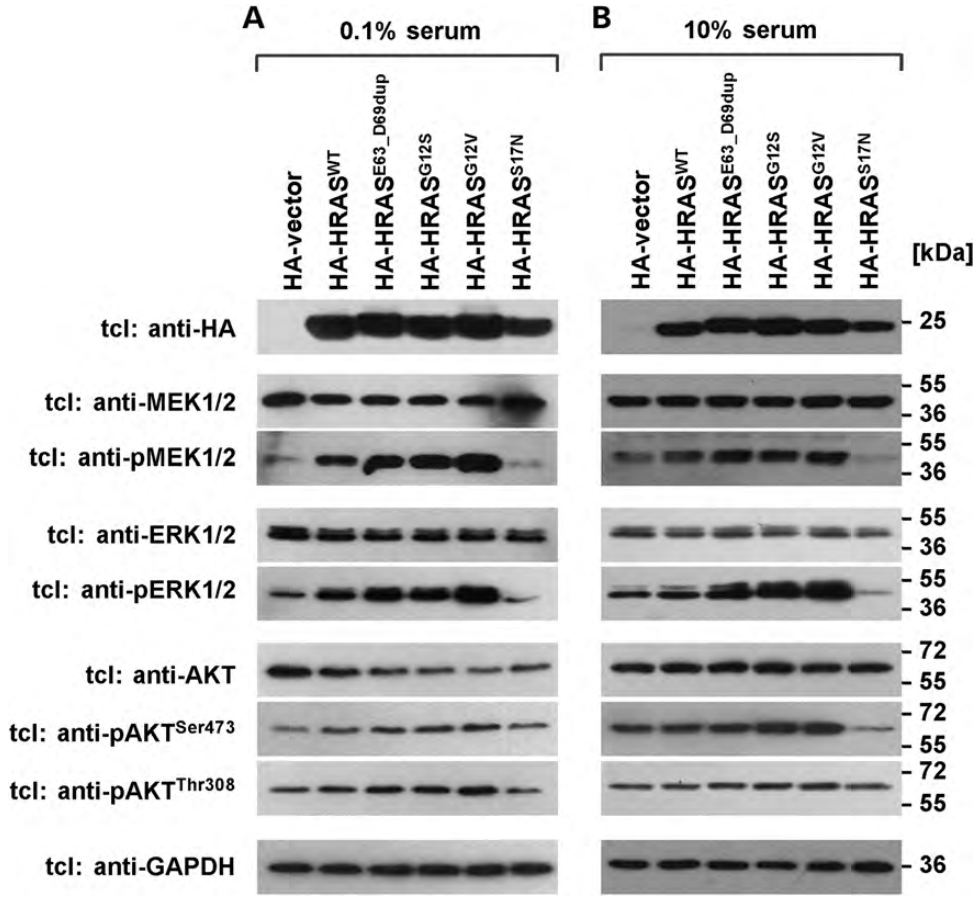

Figure 4. Expression of HRAS^{E63_D69dup} leads to enhanced phosphorylation of MEK1/2 and ERK1/2. COS-7 cells were transfected with empty vector or constructs expressing HA-HRAS^{WT}, HA-HRAS^{E63_D69dup}, HA-HRAS^{G12S}, HA-HRAS^{G12V} or HA-HRAS^{S17N} as indicated. Cells were cultured under serum-starved [0.1% serum, (A)] or basal [10% serum, (B)] conditions, and cell extracts were analyzed by immunoblotting using specific antibodies. The representative autoradiographs show levels of total MEK1/2, phospho-MEK1/2, total ERK1/2, phospho-ERK1/2, total AKT, phospho-AKT^{Ser473} and phospho-AKT^{Thr308}. Expression of HA-tagged HRAS variants in total cell extracts was demonstrated by immunoblotting using anti-HA antibody, and blots were probed with anti-GAPDH antibody to control for equal loading. tcl, total cell lysates.

has two independent molecular consequences: First, a gain-of-function effect results in the accumulation of activated HRAS^{E63_D69dup} and positively modulates RAF-MEK-ERK downstream signaling. And, second, p.E63_D69dup impairs the interaction with PIK3CA that counteracts the gain-of-function effect and leads to apparently normal PI3K-AKT signal transduction. Similarly, the Costello syndrome-associated p.E37dup mutation promotes mildly enhanced HRAS-dependent signaling that results from a balancing effect between a GAP insensitivity and inefficient effector binding (13).

If HRAS^{E63_D69dup} is constitutively active, the sensitivity for EGF-induced HRAS^{E63_D69dup} activation and the ability of HRAS^{E63_D69dup} to respond to upstream signals should be diminished or abolished. Our results, however, suggest that HRAS^{E63_D69dup} retained significant reagibility to stimuli and is still able to transmit growth factor-derived signals to MAPK cascades; this is in contrast to HRAS^{G12V} that is fully active without EGF stimulation (Fig. 5). Growth factor-independent downstream signaling is caused by HRAS mutations (p.G12V, p.G12S, p.K117R and p.A146T) that affect amino acids involved in GDP/GTP binding or guanosine triphosphate reaction (5,12,16,29). On the other side, effector/GAP binding-impaired HRAS^{E37dup} potentiated downstream signal flow only upon growth factor stimulation (13). Therefore, we suggest that the p.E63_D69dup mutation may not dramatically affect nucleotide binding or intrinsic GTP hydrolysis, but rather alters GAP/effector binding; and the latter molecular deficiencies do not fully abolish signal transducing properties of HRAS.

We observed very weak AKT phosphorylation in response to EGF stimulation both in cells expressing HRAS^{G12V} and HRAS^{E63_D69dup} (Fig. 5); however, the molecular basis for this weak AKT signaling differs between HRAS^{G12V} and HRAS^{E63_D69dup} cells: Whereas constitutive active HRAS^{G12V} results in strong hyperphosphorylation of AKT even under serum starvation and, therefore, a very weak signaling response, HRAS^{E63_D69dup} is not able to transmit upstream signaling to the PI3K-AKT cascade due to impaired PIK3K interaction.

Taken together, available data nicely demonstrate that the consequences of Costello syndrome-associated HRAS mutations on downstream signaling are variable and strongly depend on the quality of the molecular defect. In analogy, five different mechanistic classes with aberrant biochemical and

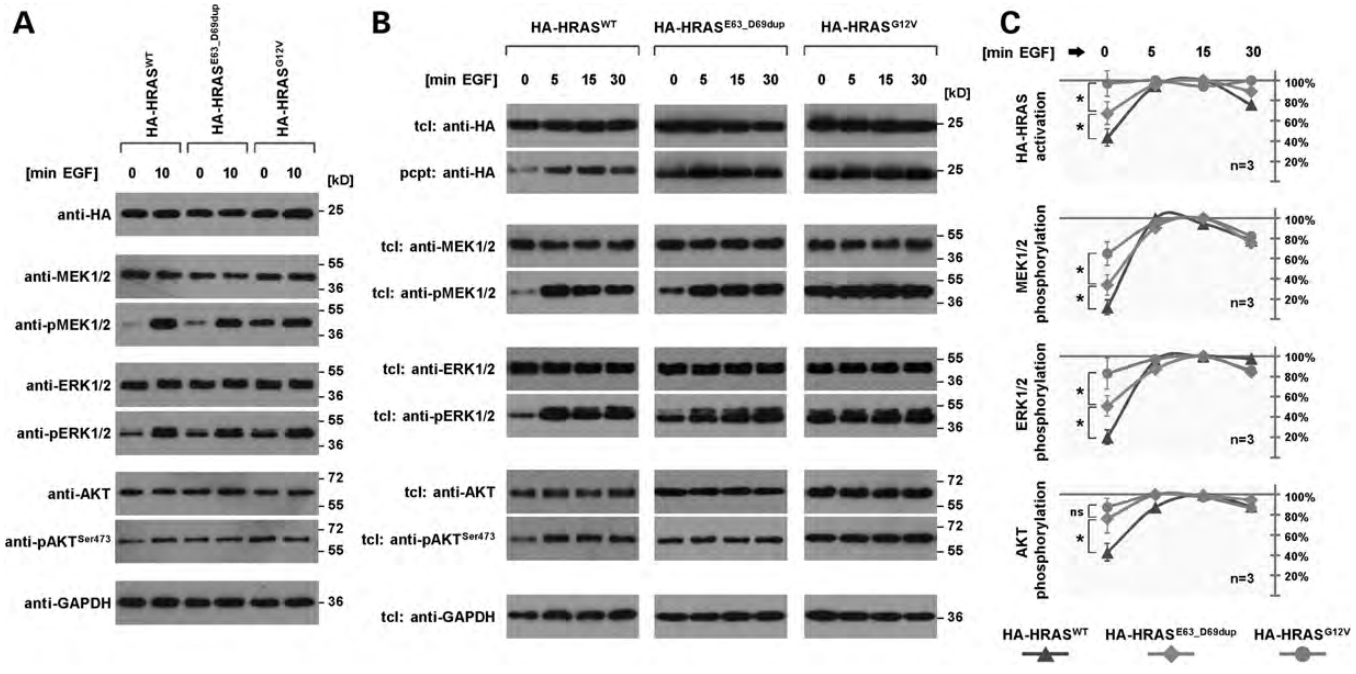

Figure 5. HRAS^{E63_D69dup} shows reduced reagibility to EGF stimulation. (**A**) COS-7 cells transiently expressing HA-HRAS^{WT}, HA-HRAS^{E63_D69dup} or HA-HRAS^{G12V} were serum starved (0.1% serum) and subsequently stimulated with 10 ng/ml EGF for 10 min or left untreated (0 min) as indicated. Cellular extracts were analyzed by immunoblotting using specific antibodies against total MEK1/2, phospho-MEK1/2, total ERK1/2, phospho-ERK1/2, total AKT and phospho-AKT^{Ser473}. Expression of HA-tagged HRAS variants in total cell extracts was demonstrated by immunoblotting using anti-HA antibody, and blots were probed with anti-GAPDH antibody to control for equal loading. (**B**) COS-7 cells transiently expressing HA-HRAS^{WT}, HA-HRAS^{E63_D69dup} or HA-HRAS^{G12V} were serum starved (0.1% serum) and subsequently stimulated with 10 ng/ml EGF for various times (5, 15, 30 min EGF) or left untreated (0 min EGF) as indicated. GTP-bound HA-HRAS was precipitated from cell extracts using GST-RAF1:RBD fusion protein. Total amounts of HA-HRAS in the total cell lysates (tcl) and precipitated HA-HRAS (pcpt) were detected using anti-HA antibody. Cellular extracts (tcl) were also analyzed by immunoblotting using specific antibodies against total MEK1/2, phospho-MEK1/2, total ERK1/2, phospho-ERK1/2, total AKT and phospho-AKT^{Ser473}. Equal loading was confirmed by immunoblotting for GAPDH. (**C**) After densitometric quantification of autoradiographic signals, levels of active HA-HRAS, phosphorylated MEK1/2, ERK1/2 and AKT were normalized relative to levels of total HA-HRAS, MEK1/2, ERK1/2 and AKT, respectively. Subsequently, maximum HA-HRAS activation levels and maximum MEK1/2, ERK1/2 and AKT phosphorylation levels were considered 100% for each stimulation series of cells expressing the indicated HRAS variants. Thus, the graphs show activation and phosphorylation levels upon 0, 5, 15 and 30 min EGF stimulation relative to maximum levels in cells expressing HRAS^{WT}, HRAS^{E63_D69dup} or HRAS^{G12V}. The number of independent experiments (n) is indicated, and the data represent the mean of n independent experiments. For untreated cells, (0 min EGF) $\pm$ standard deviation is given, and a statistical analysis was performed. Significance levels are specified between two data points on the respective curves [*, $P<0.05$; ns, statistically not significant (Student's t-test)].

physical properties have been determined for rasopathy-associated *KRAS* germline mutation (35). Our data indicate that the p.E63_D69dup mutation leads to gain-of-function of HRAS-RAF-MAPK signaling, but, concurrently, it has apparently little impact on the HRAS-PI3K-AKT signaling cascade. We suggest that both consequences are based on a massively altered HRAS^{E63_D69dup} protein topology impairing GAP binding and PI3K interaction.

Reduced reagibility, oncogenic-induced senescence and Costello syndrome

The p.E63_D69dup mutation results in a reduced reagibility to stimuli (Figs 5). In principle, constitutive hyperactivation of HRAS due to any Costello syndrome-associated or oncogenic *HRAS* mutation can be also interpreted as a reduction in HRAS reagibility to stimuli. Insensitivity to physiologic stimuli is a major characteristic of cellular senescence, a state of irreversible cellular growth arrest participating in different complex biologic processes, including tumor suppression/progression, tissue repair and aging (36). Cellular senescence can be triggered by various mechanisms such as telomere shortening, epigenetic de-repression or excess of mitogenic signals (37). The latter trigger can be delivered by certain oncogenic mutants such as the BRAF^{V600E} or the HRAS^{G12V} oncoproteins, thereby it is called oncogenic-induced senescence (38). In fact, expression of HRAS^{G12V} in a zebrafish model of Costello syndrome caused cellular senescence, but not overt constitutive activation of HRAS targets (39). Moreover, it has been demonstrated that, like HRAS^{G12V}, several other Costello-syndrome associated HRAS mutants (p.G12S, p.G12A, p.G12C, p.G12D, p.G13C, p.G13D, p.K117R and p.A146T) induce cellular senescence when overexpressed in human fibroblasts (40). The authors proposed that cellular senescence might contribute to the pathogenesis of Costello syndrome. Interestingly, results from molecular studies strongly suggest cellular senescence as one of two underlying mechanisms of pathologic premature ageing in the Hutchinson–Gilford progeria (OMIM #176670) and Werner (OMIM #277700) syndromes (reviewed in 41). Older individuals with Costello syndrome display features of premature aging such as hair loss and prematurely aged skin (1) that can also been seen in the patient presented here (Fig. 1A). Taken together, these observations may suggest that, in addition to hyperactivation of HRAS signaling

pathways, cellular senescence coupled with growth factor resistance during development may represent a second line of pathophysiology in Costello syndrome. In line with this hypothesis and based on experiments with primary fibroblasts of patients with Costello syndrome, it has been proposed that altered cellular response to growth factors rather than constitutive activation of HRAS downstream signaling molecules may contribute to the phenotype (34). This hypothesis is corroborated by the analysis of an $HRAS^{WT/G12V}$ mouse model for Costello syndrome that showed normal phosphorylation levels of Erk, Mek and Akt in all tissues tested (42). These considerations also have important implications on the research regarding future treatment strategies because inhibitors of the pathway may influence its basal activity, but not be able to restitute its dynamics.

Cell physiologic basis of phenotypic variability

The typical Costello syndrome phenotype is easily recognizable in older individuals, and it is most often due to a substitution of HRAS glycine at position 12 for a serine (1). Rarer HRAS mutations can be associated either with a more severe clinical presentation (17,43–45) or with milder findings (14,16,18). Notably, substantially attenuated clinical features are caused by mutations affecting other amino acids than glycine 12 and 13 in the P-loop of HRAS (p.Q22K, p.E37dup, p.T58I, p.E63K, p.K117R and p.A146T/V), thereby, representing the mild end of the Costello syndrome phenotype (12–17). Although it is difficult to draw definite conclusions from a single observation, the clinical expression of the syndrome in our patient suggests that the p.E63_D69dup mutation may rather belong to the latter group. Phenotypic differences of patients with Costello syndrome may mirror dissimilar molecular pathomechanisms: Whereas mutations of HRAS glycine 12 or 13 result in impaired intrinsic/GAP-stimulated GTPase activity (10), non-P-loop alterations such as $HRAS^{K117R}$ and $HRAS^{E37dup}$ are characterized by altered nucleotide binding affinities and impaired regulator/effector interaction, respectively (12,13). In line with this, $HRAS^{E63\_D69dup}$ also shows impaired regulator (NF1) and effector (PIK3CA) binding.

Because $HRAS^{E63\_D69dup}$ induces hyperstimulation of the RAF-MAPK, but not the PI3K-AKT signaling cascade, it is tempting to speculate that it is primarily the excess of RAF-MAPK signaling that underlies the Costello syndrome phenotype of our patient. However, by changing the perspective from hyperstimulation to hyporeagibility of HRAS-dependent signaling, we found both the RAF-MAPK and the PI3K-AKT cascade to be affected. Therefore, the correlation of the clinical features in our patient with the alteration of a specific signaling pathway is not possible. This is in line with other reports showing that Costello syndrome-associated HRAS alterations modify signaling via various effectors (13,34,46,47). Notably, deregulated PI3K-AKT signaling has been associated with various overgrowth syndromes such as Proteus syndrome, (hemi)megalencephaly syndromes or fibroadipose hyperplasia (48–52). Accordingly, altered PI3K-AKT signaling may underlie progressive postnatal cerebellar overgrowth and fetal overgrowth that are frequently diagnosed for patients with Costello syndrome (53,54).

The functional characterization of unusual HRAS mutations helps to put forward new hypotheses of molecular pathomechanisms and, thereby, enables a better understanding of the molecular basis of the phenotypic variability associated with pathogenic HRAS alterations. Noteworthy, a germline *HRAS* alteration (c.266C>G; p.S89C) has been previously reported in two siblings with clinical features that only marginally resemble the Costello syndrome phenotype (19). This alteration resulted in decreased EGF-induced HRAS downstream signaling that also can be interpreted as reduced reagibility/reactivity. In conclusion, available data strongly suggest that the phenotypic spectrum and the functional variability associated with germline mutations in *HRAS* will further expand in the future.

MATERIALS AND METHODS

Case presentation

The 18-year-old female patient is the offspring of a healthy, consanguineous couple (third degree cousin marriage) from Turkey. Paternal and maternal ages at conception were 38 and 25 years, respectively. The patient was born at term by normal delivery at home after an uneventful pregnancy. Her birth measurements were not recorded. The parents reported feeding difficulties and muscular hypotonia during infancy and childhood. Tube feeding was not required. The patient started to sit and to walk without support at 12 and 24 months of age, respectively. Development of speech was mildly delayed. She was admitted to a hospital with the complaints of skin lesions and easy fatigability at the age of 5 years, when she was diagnosed to have hypertrophic cardiomyopathy. She was, therefore, treated with propranolol. At the age of 8 years, osteoporosis was diagnosed, and vitamin D treatment was initiated. The patient was 13 years old, when she was first evaluated at Ihsan Dogramaci Children's Hospital. Physical examination revealed short stature with a body height of 141 cm (<3rd centile), a body weight of 33 kg (<3rd centile) and relative macrocephaly with an occipitofrontal head circumference of 55 cm (75th centile). She had coarsened facial features, bulging eyes with ptosis and hypertelorism, low-set ears, thin, sparse and curly hair, multiple lentigines particularly on the face and a relatively dark pigmentation of the skin (Fig. 1). The palms and soles were soft with deep creases. Plaque-like hyperkeratotic skin lesions were visible around her ankles. Mild skeletal abnormalities such as genu varum, pes planus and mild ulnar deviation at the wrists were also noted. Echocardiography revealed hypertrophic cardiomyopathy without obstruction, dilated coronary sinus, malalignment of the aorta and mitral and pulmonary insufficiencies. Electrocardiography demonstrated sinus tachycardia and first degree AV block. Mild intellectual disability along with good verbal communication skills was noted (a formal psychometric evaluation is not available). The patient is currently attending a regular school with additional support. She has not had any oncologic manifestations, so far. Based on the clinical features, the diagnosis of Costello syndrome was made.

Molecular genetic analysis

We collected blood samples of the patient and her parents and isolated genomic DNA from lymphocytes by standard

procedures. We amplified the coding region, including the flanking intronic sequences of the *HRAS* gene (GenBank accession nos. NM_005343.2 and NM_176795.3) from genomic DNA. Primer sequences are available on request. Mutation analysis of the amplimers was carried out by direct sequencing bidirectionally, using the ABI BigDye terminator Sequencing Kit v.3.1 (Applied Biosystems, Life Technologies, Biosystems, Weiterstadt, Germany) and an ABI 3700 Capillary Array Sequencer (Applied Biosystems). We verified the declared relationship by genotyping of the parents and the patient at 10 microsatellite loci. Ethical approval for this study was obtained, and the parents provided informed written consent for the genetic analysis.

Plasmids

We amplified the coding region of wild-type *HRAS* for the generation of an expression construct using *HRAS*-specific PCR primers and *HRAS* cDNA as a template. Mutated *HRAS* cDNA inserts [c.34G>A (p.G12S), c.35G>T (p.G12V), c.50G>A (p.S17N) and c.187_207dup (p.E63_D69dup)] were established by PCR-mediated mutagenesis. Purified PCR products were cloned into pENTR/D-TOPO (Invitrogen, Karlsruhe, Germany) according to the protocol provided. Constructs were sequenced for integrity and used for transferring wild-type and mutated *HRAS* coding regions into plasmid pMT2SM-HA-DEST (*N*-terminal HA epitope). $NF1^{333}$ in pcDNA3-FLAG contains residues 1198–1530 of human NF1 comprising the functional GAP-related domain that is able to bind to wild-type HRAS and stimulate GTP hydrolysis.

Cell culture and transfection

COS-7 cells were cultured in Dulbecco's Modified Eagle Medium (DMEM; Invitrogen) containing 10% serum (Invitrogen) and penicillin–streptomycin (100 U/ml and 100 mg/ml, respectively) (Invitrogen) at 37°C and 5% CO_2. Transfections were performed using Lipofectamine 2000 Reagent (Invitrogen) according to the manufacturer's protocol. For EGF stimulation, cells were blocked overnight by serum starvation (0.1% serum), followed by incubation in DMEM containing 10 ng/ml EGF (Sigma, Taufkirchen, Germany).

RAS activation assay

The RAS-binding domain (RBD) of RAF1 (amino acids 51–131), the RBD of PI3K (PIK3CA) (amino acids 127–314), the RAS-association (RA) domain of RALGDS (amino acids 777–872) and the RA domain of PLC1 (PLCE1) (amino acids 2130–2240) were used to specifically precipitate GTP-bound RAS proteins from cell extracts (55). Preparation of GST-RBD/RA beads, cell lysis and precipitation of GTP-bound RAS have been described elsewhere (34). After SDS PAGE and transfer to polyvinylidene difluorid (PVDF) membranes, total and precipitated (active) HA-tagged HRAS was detected using peroxidase-conjugated rat monoclonal anti-HA antibody (Roche, Mannheim, Germany; clone 3F10; 1:5000 dilution). For loading control, membranes were incubated with mouse anti-glyceraldehyde-3-phosphate dehydrogenase (GAPDH) (Abcam, Cambridge, UK; no. ab8245, 1:5000 dilution), followed by peroxidase-coupled secondary anti-mouse antibody (Amersham Pharmacia Biotech, Freiburg, Germany; no. NA9310; 1:8000 dilution).

Co-immunoprecipitation

Transiently transfected COS-7 cells were lyzed in ice-cold cell lysis buffer [150 mM Tris–HCl, pH 8.0; 50 mM NaCl; 1 mM EDTA; 0.5% Nonidet P-40; complete Mini Protease Inhibitors (Roche); 0.7 mg/ml Pepstatin] and cell extracts were clarified by centrifugation. The supernatants were transferred to 40 µl EZview™ Red Anti-HA Affinity Gel (Sigma) and incubated for 2 h at 4°C on a rotator. Precipitates were collected by repeated centrifugation and washing with cell lysis buffer, re-suspended in sample buffer (33% glycerol; 80 mM Tris–HCl, pH 6.8; 0.3 M Dithiothreitol; 6.7% sodium dodecyl sulphate; 0.1% bromophenol blue) and subjected to SDS PAGE and immunoblotting.

Immunoblotting

Twenty-four hours after transfection, cells were cultured as specified, then washed with PBS and scraped off in modified radioimmunoprecipitation assay buffer [50 mM Tris–HCl, pH 8.0; 150 mM NaCl; 1% Nonidet P-40; 0.5% sodium deoxycholate; 0.1% SDS; 1 mM phenylmethylsulfonyl fluoride; 1 mM Na_3VO_4; 10 mM NaF; 1 Complete Mini protein inhibitor cocktail tablet (Roche) per 10 ml]. Cellular biochemical reactions were stopped by freezing lysates in liquid nitrogen. After thawing on ice, cell debris was removed, and protein concentration was determined using the BCA Protein Assay Kit (Pierce, Bonn, Germany). Protein solutions were supplemented with sample buffer, and proteins were separated on SDS-polyacrylamide gels and transferred to PVDF membranes. Following blocking (20 mM Tris–HCl, pH 7.4; 150 mM NaCl; 0.1% Tween-20; 4% non-fat dry milk) and washing (20 mM Tris–HCl, pH 7.4; 150 mM NaCl; 0.1% Tween-20), membranes were incubated in primary antibody solution (20 mM Tris–HCl, pH 7.4; 150 mM NaCl; 0.1% Tween-20; 5% BSA or 0.5% non-fat dry milk) containing the appropriate antibodies. Rabbit polyclonal antibodies against MEK1/2 (Cell Signaling Tech., Danvers, MA, USA; no. 9122; 1:1000 dilution), phospho-MEK1/2 (Ser217/221) (Cell Signaling Tech.; no. 9121; 1:1000 dilution), p44/42 MAP kinase (ERK1/2) (Cell Signaling Tech.; no. 9102, 1:1000 dilution), phospho-p44/42 MAP kinase (ERK1/2) (Thr202/Tyr204) (Cell Signaling Tech.; no. 9101, 1:1000 dilution), Akt (Cell Signaling Tech.; no. 9272; 1:1000 dilution), phospho-Akt (Ser473) (Cell Signaling Tech.; no. 9271; 1:1000 dilution) and phospho-Akt (Thr308) (Cell Signaling Tech.; no. #9275; 1:1000 dilution) were used. Next, membranes were washed and incubated with peroxidase-coupled secondary anti-rabbit antibody (Amersham Pharmacia Biotech; no. NA9340V; 1:8000 dilution). After final washing, immunoreactive proteins were visualized using the Immobilon Western Chemiluminescent HRP Substrate (Millipore, Schwalbach, Germany).

Statistical analysis

Signals on autoradiographs from three independent experiments were quantified by densitometric analysis using the

ImageJ software (NIH; http://rsb.info.nih.gov/ij/index.html). MEK1/2, ERK1/2 and AKT phosphorylation as well as HRAS activation levels were assessed as described in Figure 5C. A two-tailed unpaired Student's *t*-test was used to determine the significance of the difference between cells overexpressing HRAS mutants. Values are presented as the mean ± standard deviation and were considered significant at P-value < 0.05.

GENBANK REFERENCE SEQUENCES

HRAS (HRAS, H-Ras) NM_005343.2, NM_176795.3; *MAP2K1/MAP2K2* (MEK1/2) NM_002755.3/NM_030662.2; *MAPK3/MAPK1* (ERK1/2) NM_002745.4/NM_001040056.1; *AKT1/AKT2/AKT3* (AKT1-3) NM_001014431.1/NM_0016 26.3/NM_005465.3; *GAPDH* (GAPDH) NM_002046.3; *RAF1* (CRAF, c-Raf) NM_002880.3; *RALGDS* (RalGDS, RalGEF) NM_006266.2; *PIK3CA* (PI3Ka, p110-alpha) NM_006218.2; *PLCE1* (PLC1, PLC11) NM_016341.3; *NF1* (NF1, neurofibromin 1) NM_001042492. Protein names are denoted in parentheses.

ACKNOWLEDGEMENTS

The authors are grateful to the child and her parents for their interest and participation in this study. The results summarized here are part of the MD thesis of Sybille Lorenz at the University of Hamburg, which was supervised by Kerstin Kutsche and G.R. We thank Anika Maak for generating *HRAS* c.187_207dup in pENTR/D-TOPO and Stefanie Meien for excellent technical assistance. $NF1^{333}$ in pcDNA3-FLAG was kindly provided by M. Reza Ahmadian (Institute of Biochemistry and Molecular Biology II, Heinrich Heine University Medical Center, Düsseldorf, Germany). All experiments in this study comply with the current laws of Germany (Gendiagnostikgesetz).

Conflict of Interest statement. None declared.

FUNDING

This work was supported by grants from the Werner-Otto-Stiftung (Beschluss Nr. 4/77) to G.R. and from the European Research Area Network for research programs on rare diseases (E-Rare) 2009 to M.Z.

REFERENCES

1. Gripp, K.W. and Lin, A. (2006) Costello Syndrome. 2006 Aug 29 [Updated 2012 Jan 12]. In Pagon, RA, Bird, TD, Dolan, CR *et al.* (eds), *GeneReviews*™ [Internet]. University of Washington, Seattle, Seattle, WA, pp. 1993–2012. Available from: http://www.ncbi.nlm.nih.gov/books/NBK1507/. Accessed August 20, 2012.
2. Aoki, Y., Niihori, T., Kawame, H., Kurosawa, K., Ohashi, H., Tanaka, Y., Filocamo, M., Kato, K., Suzuki, Y., Kure, S. *et al.* (2005) Germline mutations in HRAS proto-oncogene cause Costello syndrome. *Nat. Genet.*, **37**, 1038–1040.
3. Guo, Z., Ahmadian, M.R. and Goody, R.S. (2005) Guanine nucleotide exchange factors operate by a simple allosteric competitive mechanism. *Biochemistry*, **44**, 15423–15429.
4. Scheffzek, K. and Ahmadian, M.R. (2005) GTPase activating proteins: structural and functional insights 18 years after discovery. *Cell. Mol. Life Sci.*, **62**, 3014–3038.
5. Karnoub, A.E. and Weinberg, R.A. (2008) Ras oncogenes: split personalities. *Nat. Rev. Mol. Cell Biol.*, **9**, 517–531.
6. Sol-Church, K. and Gripp, K.W. (2009) The molecular basis of Costello syndrome. In Zenker, M. (ed), *Noonan Syndrome and Related Disorders – A Matter of Deregulated Ras Signaling*. Karger, Basel, pp. 94–103.
7. Gripp, K.W., Lin, A.E., Stabley, D.L., Nicholson, L., Scott, C.I. Jr, Doyle, D., Aoki, Y., Matsubara, Y., Zackai, E.H., Lapunzina, P. *et al.* (2006) HRAS mutation analysis in Costello syndrome: genotype and phenotype correlation. *Am. J. Med. Genet. A*, **140A**, 1–7.
8. Fasano, O., Aldrich, T., Tamanoi, F., Taparowsky, E., Furth, M. and Wigler, M. (1984) Analysis of the transforming potential of the human H-ras gene by random mutagenesis. *Proc. Natl. Acad. Sci. USA*, **81**, 4008–4012.
9. Gideon, P., John, J., Frech, M., Lautwein, A., Clark, R., Scheffler, J.E. and Wittinghofer, A. (1992) Mutational and kinetic analyses of the GTPase-activating protein (GAP)-p21 interaction: the C-terminal domain of GAP is not sufficient for full activity. *Mol. Cell. Biol.*, **12**, 2050–2056.
10. Scheffzek, K., Ahmadian, M.R., Kabsch, W., Wiesmuller, L., Lautwein, A., Schmitz, F. and Wittinghofer, A. (1997) The Ras-RasGAP complex: structural basis for GTPase activation and its loss in oncogenic Ras mutants. *Science*, **277**, 333–338.
11. Seeburg, P.H., Colby, W.W., Capon, D.J., Goeddel, D.V. and Levinson, A.D. (1984) Biological properties of human c-Ha-ras1 genes mutated at codon 12. *Nature*, **312**, 71–75.
12. Denayer, E., Parret, A., Chmara, M., Schubbert, S., Vogels, A., Devriendt, K., Frijns, J.P., Rybin, V., de Ravel, T.J., Shannon, K. *et al.* (2008) Mutation analysis in Costello syndrome: functional and structural characterization of the HRAS p.Lys117Arg mutation. *Hum. Mutat.*, **29**, 232–239.
13. Gremer, L., De Luca, A., Merbitz-Zahradnik, T., Dallapiccola, B., Morlot, S., Tartaglia, M., Kutsche, K., Ahmadian, M.R. and Rosenberger, G. (2010) Duplication of Glu37 in the switch I region of HRAS impairs effector/GAP binding and underlies Costello syndrome by promoting enhanced growth factor-dependent MAPK and AKT activation. *Hum. Mol. Genet.*, **19**, 790–802.
14. Gripp, K.W., Innes, A.M., Axelrad, M.E., Gillan, T.L., Parboosingh, J.S., Davies, C., Leonard, N.J., Lapointe, M., Doyle, D., Catalano, S. *et al.* (2008) Costello syndrome associated with novel germline HRAS mutations: an attenuated phenotype? *Am. J. Med. Genet. A*, **146A**, 683–690.
15. Kerr, B., Delrue, M.A., Sigaudy, S., Perveen, R., Marche, M., Burgelin, I., Stef, M., Tang, B., Eden, O.B., O'Sullivan, J. *et al.* (2006) Genotype-phenotype correlation in Costello syndrome: HRAS mutation analysis in 43 cases. *J. Med. Genet.*, **43**, 401–405.
16. Zampino, G., Pantaleoni, F., Carta, C., Cobellis, G., Vasta, I., Neri, C., Pogna, E.A., De Feo, E., Delogu, A., Sarkozy, A. *et al.* (2007) Diversity, parental germline origin, and phenotypic spectrum of de novo HRAS missense changes in Costello syndrome. *Hum. Mutat.*, **28**, 265–272.
17. van der Burgt, I., Kupsky, W., Stassou, S., Nadroo, A., Barroso, C., Diem, A., Kratz, C.P., Dvorsky, R., Ahmadian, M.R. and Zenker, M. (2007) Myopathy caused by HRAS germline mutations: implications for disturbed myogenic differentiation in the presence of constitutive HRas activation. *J. Med. Genet.*, **44**, 459–462.
18. Gripp, K.W., Hopkins, E., Sol-Church, K., Stabley, D.L., Axelrad, M.E., Doyle, D., Dobyns, W.B., Hudson, C., Johnson, J., Tenconi, R. *et al.* (2011) Phenotypic analysis of individuals with Costello syndrome due to HRAS p.G13C. *Am. J. Med. Genet. A*, **155A**, 706–716.
19. Gripp, K.W., Bifeld, E., Stabley, D.L., Hopkins, E., Meien, S., Vinette, K., Sol-Church, K. and Rosenberger, G. (2012) A novel HRAS substitution (c.266C>G; p.S89C) resulting in decreased downstream signaling suggests a new dimension of RAS pathway dysregulation in human development. *Am. J. Med. Genet. A*, **158A**, 2106–2118.
20. Kerr, B. (2009). In Zenker, M. (ed), The clinical phenotype of Costello syndrome. In *Noonan Syndrome and Related Disorders – A Matter of Deregulated Ras Signaling*. Karger, Basel, pp. 83–93.
21. Vetter, I.R. and Wittinghofer, A. (2001) The guanine nucleotide-binding switch in three dimensions. *Science*, **294**, 1299–1304.
22. Boriack-Sjodin, P.A., Margarit, S.M., Bar-Sagi, D. and Kuriyan, J. (1998) The structural basis of the activation of Ras by Sos. *Nature*, **394**, 337–343.

23. Polakis, P. and McCormick, F. (1993) Structural requirements for the interaction of p21ras with GAP, exchange factors, and its biological effector target. *J. Biol. Chem.*, **268**, 9157–9160.
24. Stieglitz, B., Bee, C., Schwarz, D., Yildiz, O., Moshnikova, A., Khokhlatchev, A. and Herrmann, C. (2008) Novel type of Ras effector interaction established between tumour suppressor NORE1A and Ras switch II. *EMBO J.*, **27**, 1995–2005.
25. Farnsworth, C.L. and Feig, L.A. (1991) Dominant inhibitory mutations in the Mg(2+)-binding site of RasH prevent its activation by GTP. *Mol. Cell. Biol.*, **11**, 4822–4829.
26. Stacey, D.W., Feig, L.A. and Gibbs, J.B. (1991) Dominant inhibitory Ras mutants selectively inhibit the activity of either cellular or oncogenic Ras. *Mol. Cell. Biol.*, **11**, 4053–4064.
27. Ahmadian, M.R., Kiel, C., Stege, P. and Scheffzek, K. (2003) Structural fingerprints of the Ras-GTPase activating proteins neurofibromin and p120GAP. *J. Mol. Biol.*, **329**, 699–710.
28. Scheffzek, K., Ahmadian, M.R., Wiesmuller, L., Kabsch, W., Stege, P., Schmitz, F. and Wittinghofer, A. (1998) Structural analysis of the GAP-related domain from neurofibromin and its implications. *EMBO J.*, **17**, 4313–4327.
29. Schubbert, S., Shannon, K. and Bollag, G. (2007) Hyperactive Ras in developmental disorders and cancer. *Nat. Rev. Cancer*, **7**, 295–308.
30. Pacold, M.E., Suire, S., Perisic, O., Lara-Gonzalez, S., Davis, C.T., Walker, E.H., Hawkins, P.T., Stephens, L., Eccleston, J.F. and Williams, R.L. (2000) Crystal structure and functional analysis of Ras binding to its effector phosphoinositide 3-kinase gamma. *Cell*, **103**, 931–943.
31. Walker, E.H., Perisic, O., Ried, C., Stephens, L. and Williams, R.L. (1999) Structural insights into phosphoinositide 3-kinase catalysis and signalling. *Nature*, **402**, 313–320.
32. Moodie, S.A., Paris, M., Villafranca, E., Kirshmeier, P., Willumsen, B.M. and Wolfman, A. (1995) Different structural requirements within the switch II region of the Ras protein for interactions with specific downstream targets. *Oncogene*, **11**, 447–454.
33. Bunney, T.D., Harris, R., Gandarillas, N.L., Josephs, M.B., Roe, S.M., Sorli, S.C., Paterson, H.F., Rodrigues-Lima, F., Esposito, D., Ponting, C.P. *et al.* (2006) Structural and mechanistic insights into ras association domains of phospholipase C epsilon. *Mol. Cell*, **21**, 495–507.
34. Rosenberger, G., Meien, S. and Kutsche, K. (2009) Oncogenic HRAS mutations cause prolonged PI3K signaling in response to epidermal growth factor in fibroblasts of patients with Costello syndrome. *Hum. Mutat.*, **30**, 352–362.
35. Gremer, L., Merbitz-Zahradnik, T., Dvorsky, R., Cirstea, I.C., Kratz, C.P., Zenker, M., Wittinghofer, A. and Ahmadian, M.R. (2010) Germline KRAS mutations cause aberrant biochemical and physical properties leading to developmental disorders. *Hum. Mutat.*, **32**, 33–43.
36. Rodier, F. and Campisi, J. (2011) Four faces of cellular senescence. *J. Cell Biol.*, **192**, 547–556.
37. Collado, M., Blasco, M.A. and Serrano, M. (2007) Cellular senescence in cancer and aging. *Cell*, **130**, 223–233.
38. Gorgoulis, V.G. and Halazonetis, T.D. (2010) Oncogene-induced senescence: the bright and dark side of the response. *Curr. Opin. Cell Biol.*, **22**, 816–827.
39. Santoriello, C., Deflorian, G., Pezzimenti, F., Kawakami, K., Lanfrancone, L., d'Adda di Fagagna, F. and Mione, M. (2009) Expression of H-RASV12 in a zebrafish model of Costello syndrome causes cellular senescence in adult proliferating cells. *Dis. Model Mech.*, **2**, 56–67.
40. Niihori, T., Aoki, Y., Okamoto, N., Kurosawa, K., Ohashi, H., Mizuno, S., Kawame, H., Inazawa, J., Ohura, T., Arai, H. *et al.* (2011) HRAS mutants identified in Costello syndrome patients can induce cellular senescence: possible implications for the pathogenesis of Costello syndrome. *J. Hum. Genet.*, **56**, 707–715.
41. Dominguez-Gerpe, L. and Araujo-Vilar, D. (2008) Prematurely aged children: molecular alterations leading to Hutchinson-Gilford progeria and Werner syndromes. *Curr. Aging Sci.*, **1**, 202–212.
42. Schuhmacher, A.J., Guerra, C., Sauzeau, V., Canamero, M., Bustelo, X.R. and Barbacid, M. (2008) A mouse model for Costello syndrome reveals an Ang II-mediated hypertensive condition. *J. Clin. Invest.*, **118**, 2169–2179.
43. Lin, A.E., O'Brien, B., Demmer, L.A., Almeda, K.K., Blanco, C.L., Glasow, P.F., Berul, C.I., Hamilton, R., Micheil Innes, A., Lauzon, J.L. *et al.* (2009) Prenatal features of Costello syndrome: ultrasonographic findings and atrial tachycardia. *Prenat. Diagn.*, **29**, 682–690.
44. Lo, I.F., Brewer, C., Shannon, N., Shorto, J., Tang, B., Black, G., Soo, M.T., Ng, D.K., Lam, S.T. and Kerr, B. (2008) Severe neonatal manifestations of Costello syndrome. *J. Med. Genet.*, **45**, 167–171.
45. Lorenz, S., Petersen, C., Kordass, U., Seidel, H., Zenker, M. and Kutsche, K. (2012) Two cases with severe lethal course of Costello syndrome associated with HRAS p.G12C and p.G12D. *Eur. J. Med. Genet.*, **55**, 615–619.
46. Yan, J., Roy, S., Apolloni, A., Lane, A. and Hancock, J.F. (1998) Ras isoforms vary in their ability to activate Raf-1 and phosphoinositide 3-kinase. *J. Biol. Chem.*, **273**, 24052–24056.
47. Li, W., Zhu, T. and Guan, K.L. (2004) Transformation potential of Ras isoforms correlates with activation of phosphatidylinositol 3-kinase but not ERK. *J. Biol. Chem.*, **279**, 37398–37406.
48. Lindhurst, M.J., Parker, V.E., Payne, F., Sapp, J.C., Rudge, S., Harris, J., Witkowski, A.M., Zhang, Q., Groeneveld, M.P., Scott, C.E. *et al.* (2012) Mosaic overgrowth with fibroadipose hyperplasia is caused by somatic activating mutations in PIK3CA. *Nat. Genet.*, **44**, 928–933.
49. Poduri, A., Evrony, G.D., Cai, X., Elhosary, P.C., Beroukhim, R., Lehtinen, M.K., Hills, L.B., Heinzen, E.L., Hill, A., Hill, R.S. *et al.* (2012) Somatic activation of AKT3 causes hemispheric developmental brain malformations. *Neuron*, **74**, 41–48.
50. Lee, J.H., Huynh, M., Silhavy, J.L., Kim, S., Dixon-Salazar, T., Heiberg, A., Scott, E., Bafna, V., Hill, K.J., Collazo, A. *et al.* (2012) De novo somatic mutations in components of the PI3K-AKT3-mTOR pathway cause hemimegalencephaly. *Nat. Genet.*, **44**, 941–945.
51. Riviere, J.B., Mirzaa, G.M., O'Roak, B.J., Beddaoui, M., Alcantara, D., Conway, R.L., St-Onge, J., Schwartzentruber, J.A., Gripp, K.W., Nikkel, S.M. *et al.* (2012) De novo germline and postzygotic mutations in AKT3, PIK3R2 and PIK3CA cause a spectrum of related megalencephaly syndromes. *Nat. Genet.*, **44**, 934–940.
52. Lindhurst, M.J., Sapp, J.C., Teer, J.K., Johnston, J.J., Finn, E.M., Peters, K., Turner, J., Cannons, J.L., Bick, D., Blakemore, L. *et al.* (2011) A mosaic activating mutation in AKT1 associated with the Proteus syndrome. *New Engl. J. Med.*, **365**, 611–619.
53. Gripp, K.W., Hopkins, E., Doyle, D. and Dobyns, W.B. (2010) High incidence of progressive postnatal cerebellar enlargement in Costello syndrome: brain overgrowth associated with HRAS mutations as the likely cause of structural brain and spinal cord abnormalities. *Am. J. Med. Genet. A*, **152A**, 1161–1168.
54. Smith, L.P., Podraza, J. and Proud, V.K. (2009) Polyhydramnios, fetal overgrowth, and macrocephaly: prenatal ultrasound findings of Costello syndrome. *Am. J. Med. Genet. A*, **149A**, 779–784.
55. de Rooij, J. and Bos, J.L. (1997) Minimal Ras-binding domain of Raf1 can be used as an activation-specific probe for Ras. *Oncogene*, **14**, 623–625.
56. Wennerberg, K., Rossman, K.L. and Der, C.J. (2005) The Ras superfamily at a glance. *J. Cell Sci.*, **118**, 843–846.